

A comparison between coral colonies of the genus *Madracis* and simulated forms.



Journal:	<i>Proceedings B</i>
Manuscript ID:	Draft
Article Type:	Research
Date Submitted by the Author:	n/a
Complete List of Authors:	Filatov, M.; University of Amsterdam, Section Computational Science Kaandorp, J.; University of Amsterdam, Section Computational Science Postma, M.; University of Amsterdam, Section Computational Science Vermeij, M.; Carmabi Foundation; University of Amsterdam, IBED Bak, R.; Netherlands Institute of Sea Research, Marine Ecology van Liere, R.; Center for Mathematics and Computer Science Streekstra, G.; Academic medical center, Biomedical Engineering and Physics Kruszynski, Krzysztof; Center for Mathematics and Computer Science
Subject:	Ecology < BIOLOGY, Systems Biology < BIOLOGY, Biomechanics < BIOLOGY
Keywords:	scleractinian corals, simulation, morphology, <i>Madracis</i> , Computed Tomography scans, morphogenesis
Proceedings B category:	Theoretical Biology



1 **A comparison between coral colonies of the genus**
2 ***Madracis* and simulated forms.**

3 Maxim V. Filatov¹, Jaap A. Kaandorp¹, Marten Postma¹, Robert van Liere², Kris J.
4 Kruszyński², Mark J.A. Vermeij^{3,4}, Geert J. Streekstra⁵ and Rolf P.M. Bak⁶

5
6 1. Section Computational Science, Faculty of Science, University of Amsterdam
7 Science Park 107
8 1098 XG Amsterdam
9 The Netherlands

10 Corresponding author email: J.A.Kaandorp@uva.nl

11
12 2. Center for Mathematics and Computer Science
13 Kruislaan 413
14 1098 SJ Amsterdam
15 The Netherlands

16
17 3. Carmabi Foundation
18 Piscaderabaai z/n
19 Curaçao, Netherlands Antilles

20
21
22 4. IBED, University of Amsterdam
23 Nieuwe Achtergracht 127,
24 1018 WS Amsterdam
25 The Netherlands

26
27 5. Academic Medical Center
28 Dept. Biomedical Engineering and Physics
29 Meibergdreef 9
30 1105 AZ Amsterdam
31 The Netherlands

32
33 6. Dept of Marine Ecology
34 Netherlands Institute of Sea Research (NIOZ)
35 P.O. Box 59
36 1790 AB Den Burg
37 The Netherlands

38 Abstract

39 In addition to experimental studies, computational models provide valuable information about
40 colony development in scleractinian corals. Using our simulation model we show how
41 environmental factors such as nutrient distribution and light availability affect growth patterns
42 of coral colonies. To compare the simulated coral growth forms with those of real coral
43 colonies, we quantitatively compared our modeling results with coral colonies of the
44 morphologically variable Caribbean coral genus *Madracis*. *Madracis* species encompass a
45 relatively large morphological variation in colony morphology and hence represents a suitable
46 genus to, for the first time, compare simulated and real coral growth forms in 3D using a
47 quantitative approach. This quantitative analysis of three-dimensional growth forms is based
48 on a number of morphometric parameters such as branch thickness, branch spacing etc. Our
49 results show that simulated coral morphologies share several morphological features with real
50 coral colonies (*M. mirabilis*, *M. decactis*, *M. formosa* and *M. carmabi*). A significant
51 correlation was found between branch thickness and branch spacing for both real and
52 simulated growth forms. Our present model is able to partly capture the morphological
53 variation in closely related and morphologically variable coral species of the genus *Madracis*.

54 **Keywords:** corals; morphogenesis; morphology; simulation; CT-scan; *Madracis*;

55

56 1. Introduction

57 Scleractinian corals exhibit great inter- and intraspecific variation in coral colony
58 morphology (e.g., Veron 1995; Bruno & Edmunds 2007). Intra-specific variation often arises
59 from plasticity in a colony's growth process in response to variable environmental conditions,
60 such as flow speed, availability of light and the availability dissolved inorganic carbon (Muko

61 2000; Todd et. al. 2004; Todd 2008). Because genetic and environmental factors determine a
62 colony's three-dimensional structure, the relative importance of either factor is often difficult
63 to determine. Experimental studies whereby corals are grown under different environmental
64 conditions are often limited by the slow growth rates of corals and difficulties with controlling
65 environmental parameters of the system. Therefore, plastic responses to environmental
66 changes are studied in relatively few (about 17) coral species (Todd 2008).

67 To determine the degree of phenotypic plasticity among colonies of the same species
68 under variable environmental conditions, various morphometric traits are measured to
69 quantitatively assess whether changes in coral colony growth and form correlate with varying
70 environmental factors (e.g., Bruno & Edmunds, 1997). Morphological variation in corals
71 exists on different scales, i.e. from differences in corallite structure within a single colony
72 (Foster, 1979) to variation among colonies in a single species. The present study aims to
73 describe variability at the colony morphology level in species of the Caribbean coral genus
74 *Madracis*. Morphological traits such as the branch diameter and branch spacing in *M.*
75 *mirabilis* are under the influence of the environment (Bruno & Edmunds, 1997). Other corals,
76 such as *Stylophora pistilata* and *Acropora eurystoma* also tend to have a certain degree of
77 phenotypic plasticity (Shaish, 2007; Bongiorni et. al., 2003). Some corals, on the other hand,
78 show very little or no phenotypic response to environment, e.g. *Pavona cactus* (Willis, 1985)
79 suggesting that in this species colony morphology is primarily driven by genetic factors.

80 Computational models support the evidence of phenotypic plasticity found in
81 biological experiments. The amount of light and nutrient distribution have been used to
82 simulate a range of coral morphologies under different environmental conditions (Muko et. al.
83 2000; Graus & McIntyre 1982; Kaandorp & Kübler, 2001; Merks et al., 2004; Kaandorp et
84 al., 2005). Using a computational approach, Kaandorp et al. (2005) found that gradients in
85 dissolved inorganic carbon (DIC) around coral colonies are responsible for branching colony

86 morphologies. A field experiment to investigate the same phenomenon would be practically
87 impossible due to the slow growth of colonies in the field and problems associated with
88 measuring DIC at the sub mm scale as used in the computational study. Therefore, in addition
89 to field experiments, computational models are an important alternative to study processes at
90 very different time and spatial scales.

91 Here we validate the previously-developed coral growth model (Merks et al 2004) that
92 combines the effects of variable environmental parameters with variation in species-specific
93 information, i.e. distance between polyps and polyp height (Kaandorp et al., 2005). The
94 model is suitable for simulating corals that have undifferentiated polyps (e.g. *Madracis*
95 species), i.e., there is no differentiation in axial and radial polyps in *M. mirabilis* colonies.
96 This unlike for example *Acropora* species, where a fast growing axial polyp occurs at the tip
97 of each branch (Wallace, 1999) differs from the other (radial) polyps on the same branch. The
98 simulations produced by the growth model produce morphologies that resemble the shape of
99 coral colonies belonging to the Caribbean coral species *Madracis mirabilis* (figure 1a). In
100 general, objects generated by the model can be characterized by very regular branch spacing.
101 This makes them suitable for comparison with real colonies of *M. mirabilis* (figure 1a) that
102 show similar regular branch spacing.

103 Verification of the model by quantitative comparison of colony morphologies between
104 simulation results and real coral colonies is crucial for further exploration of factors involved
105 in coral colony development. For a comparative analysis we can use quantitative
106 measurements of such morphological traits as branch spacing, branch thickness, branching
107 angle and branching rate of real coral colonies and simulated growth forms. A recently
108 developed morphometric method is using high resolution Computed Tomography (CT) scans
109 of coral colonies to provide such information (Kruszynski et al., 2007). In the present
110 manuscript a quantitative morphological analysis is applied to a range of simulated

111 morphologies and to CT-scans of real colonies of several coral species belonging to the genus
112 *Madracis*, i.e. *M. decactis*, *M. carmabi*, *M. formosa*, and *M. mirabilis*. The relation between
113 several morphological traits of the coral colonies will be investigated. This quantitative
114 approach allows for classification of the coral morphologies based on the shape of the colony.
115 We will demonstrate that coral morphologies can be classified using a set of morphometric
116 traits.

117 **2. Materials and methods**

118 ***Data acquisition***

119 *M. mirabilis* (n = 3), *M. carmabi* (n = 10), *M. decactis* (n = 10) and *M. formosa* (n =
120 7) colonies were collected at depths between 6 m to 50 m on Curaçao (Netherlands Antilles,
121 12° N, 69° W). 3D images of these colonies were obtained using CT scanning techniques
122 (Kaandorp, and Kübler 2001). The CT scans were made at a resolution with a voxel (i.e.
123 volumetric pixel) size of 0.33 mm × 0.33 mm × 1.50 mm (*M. carmabi*, *M. decactis* and *M.*
124 *formosa*) and almost isotropic voxel size of 0.25 mm × 0.25 mm × 0.30 mm (*M. mirabilis*).
125 The number of slices per colony varies between 45 and 765 depending on overall colony size.
126 The 3D data was edited (the substrate plate on which samples were lying was cropped) and
127 visualized using the open source OsiriX Imaging Software. In figure 1 these datasets are
128 visualized using volume rendering. Three-dimensional objects generated by 3D surface
129 rendering are used for the morphometric analyses described below.

130 ***Morphometrics***

131 By using Computed Tomography scans in morphometric software (Kruszynski et al,
132 2007), some of the key morphometric features of the coral colonies can be measured.
133 Morphometric analyses start with the construction of a morphological skeleton of each 3D

134 object, which consists of the medial axis of each branch, shown in figure 2a. This is done by
 135 the skeletonization algorithm described in Kruszynski et al. (2007).

136 By combining volumetric information and the morphological skeleton derived from
 137 the medial axis it is possible to measure the following morphological parameters. Branch
 138 thickness at the beginning of a branching point is defined by the diameter (da) of the white
 139 sphere in figure 2b. The diameter (db) of the black sphere, figure 2b, defines the branch
 140 thickness after branching. The diameter (dc) of the grey sphere located at the end point of a
 141 branch defines the thickness of a branch tip. Branching angle, (b_angle), is measured between
 142 the lines connecting center points of the a -sphere (white) and b -spheres (black). Branching
 143 angle relative to the growth direction, (g_angle), is measured between the positive y -axis and
 144 a branch, figure 2d. Branching rate, (rb), is defined as the length of the edge connecting two
 145 successive a -spheres. Branch spacing, ($br_spacing$), is equal to the radius of a sphere centred
 146 at the branch tip, which reaches the closest branch (figure 2c). The same morphological
 147 features were measured in simulated objects to allow a comparison of these parameters
 148 between simulated and real coral colonies. More detailed information about the algorithms
 149 used by the morphometric software can be found in Kruszynski et al. (2007).

150 ***Simulations with the accretive growth model***

151 An accretive growth model was used to simulate coral morphologies (Merks et al.
 152 2003, Kaandorp et al, 2005). The model simulates the growth of the colony skeleton as an
 153 accretive process whereby subsequent growth layers are deposited on top of the previous one
 154 as the coral colony grows. The geometry of each layer is represented by a triangulated
 155 surface. The distance l between the two layers, i.e. skeleton thickness, is assumed to be
 156 linearly dependent on the amount of absorbed nutrients and local light intensity as follows:

$$157 \quad l = (1 - \alpha)nc_i^{\text{nutrient}} + \alpha c_i^{\text{light}}, 0 \leq \alpha \leq 1 \quad (2.1)$$

158

159 where \bar{h} denotes the average normal at vertex i , c_i denotes the amount of absorbed nutrients or
160 light and α denotes the parameter controlling relative contribution of light intensity and
161 nutrient concentration to the growth process.

162 The main assumption made in the model is that the growth of the skeleton is limited
163 by the amount of local availability of dissolved inorganic carbon (DIC) and light in the
164 environment. Higher DIC availability promotes calcification depending on light availability
165 (Gattuso et al., 1999). Branching in the simulated object emerges from competition between
166 the polyps for available nutrients (Merks et al, 2004).

167 The simulation occurs within a three-dimensional volume, i.e. simulation box (figure
168 3). As an initial object, a sphere, is placed in the middle of the volume on the bottom plane.
169 Simulated DIC propagates through the volume by means of diffusion. The top plane of the
170 simulation box acts as source and the bottom plane and the surface of the simulated object as
171 a sink for nutrients. The diffusion is modelled using the lattice Boltzmann method (Chopard
172 & Droz 1998; Succi 2001). The nutrient distribution is recomputed after each growth step of
173 the simulated object. Different boundary conditions can be applied: nutrient source at the top
174 plane or additional nutrient source from all four side planes. These conditions were assumed
175 to represent situations whereby the nutrient supply towards an isolated, simulated colony
176 occurs with or without competition from neighbouring colonies respectively.

177 The model uses several species-specific parameters such as distance between polyps
178 and polyp height. The latter is modelled by the absorption of nutrients at a short distance from
179 the skeleton surface. By varying environmental modelling parameters such as light intensity,
180 nutrient availability and the degree of diffusion of the nutrients across the object surface, we
181 simulate various morphologies. The translocation of absorbed nutrients between the
182 neighbouring polyps is modelled by lateral diffusion across the surface of the object:

$$183 \quad \frac{\partial c(x,t)}{\partial t} = D\nabla^2 c(x,t) \quad (2.2)$$

184 where c is the concentration of nutrients at point x and time t and D the diffusion coefficient.

185 ***Measurements***

186 The quantification of the morphometric parameters of the simulated corals and CT-
187 scans is presented as a series of histograms (see supplementary information). Every branch,
188 branching angle and other features are measured for each colony resulting in a large number
189 (order of 100) of measurements per colony. For each colony a distribution of each measured
190 morphological trait (e.g. branch thickness) is calculated. Consecutive morphological analysis
191 is carried out based on these distributions.

192 ***Statistical analyses***

193 Data were normalized to allow the comparison of dimensionless descriptors of real and
194 simulated coral morphologies. Additionally, outliers were removed using the ESD many-
195 outlier procedure ($k=3$, $\alpha=0.05$; Rosner, 1983). Correlation analyses were used to detect
196 relationships among the descriptors of colonies' morphological traits. The correlation matrix
197 between all measured parameters and corresponding p-values can be found in the
198 supplementary material. Scatter plots for all pairs of variables are presented in the
199 supplementary material (figure A.3). For comparison between real and simulated coral
200 morphologies we use multivariate data analyses. We carried out a principal component
201 analysis (PCA), discriminant analysis (DA) and multivariate analysis of variance (MANOVA)
202 methods on normalized variables. DA was used to classify samples with quadratic
203 discriminant function. Multidimensional scaling (MDS) was also applied on the distance
204 matrix to visualize dissimilarities between the samples in the Euclidean 2D-space.

205

206 3. Results

207 The range of simulated coral morphologies in response to interacting levels of light
208 and nutrient diffusion across the coral colony's surface is given in figure 4. By gradually
209 increasing the values of two model parameters for light intensity and surface diffusion, thin-
210 branched morphologies are transformed into more compact growth forms.

211 A complete overview of all measured morphological traits of the simulations and real
212 coral colonies can be found in the supplementary material (A.8 Histograms). We found three
213 significantly ($p < 0.0001$) correlated variables in both simulated and real shapes. The strongest
214 linear correlation ($r = 0.73$, $p < 0.0001$) was observed between branch spacing (*br_spacing*)
215 and branching rate (*rb*). Branching rate (*rb*) is also correlated ($r = 0.68$, $p < 0.0001$) with
216 branch thickness (*db*). In addition to linear correlation ($r = 0.67$, $p < 0.0001$) between branch
217 thickness (*db*) and branch spacing (*br_spacing*), a scatter plot of these two variables (figure 5)
218 shows that species tend to group more among each other than with colonies of other species.
219 Scatter plots and correlation coefficients of all other variables can be found in the
220 supplementary material (A3).

221 Morphological variation is illustrated using a PCA scatter plot for the first two
222 principal components (PC1 and PC2) (figure 6). The simulations and *M. mirabilis* species are
223 mostly discriminated from the other species by the first principal component. PC1 and PC2
224 together describe 68% of variance in the dataset. Other principal components are not
225 sufficient for the discrimination of the samples. A discriminant analysis applied to the first
226 two PCs shows the classification of the species and simulations (see supplementary material
227 A6).

228 By testing different subsets of variables we found that, three morphological traits are
229 most suitable to discriminate between different coral species: the thickness in the middle of

230 the branch (*db*), branch spacing (*br_spacing*) and the ratio *da/rb*. A visualization of this
231 parameter space with MDS is presented in the supplementary material in figure A.5.

232 The significance of the dissimilarities between the species (including simulations) was
233 analyzed using MANOVA. The number of dimensions containing group means was $d=2$
234 ($\alpha=1\%$, $p<<0.001$). Therefore, we used first two canonical vectors (CVs) to visualize the
235 results. The MANOVA plot of the first two canonical vectors is presented in figure 7.

236 Simulations form a close group with two outliers (*env1-0* and *env1-002*). Real corals (except
237 for *M. mirabilis*) form a group with *M. formosa* in the middle and *M. carmabi* and *M. decactis*
238 on the separate ends of the group. *M. mirabilis* lies between the simulations and other coral
239 species. The group that lies the closest to the simulations is *M. mirabilis*. A discriminant
240 analysis applied to the first two canonical vectors (CV) shows the classification of the species
241 and simulations (see supplementary material A7).

242

243 4. Discussion

244

245 The comparative morphological analysis between simulations and real coral colonies
246 shows that simulated forms share three morphological features with *Madracis* species
247 described in this paper. Branch thickness (*db*), branching rate (*rb*) and branch spacing
248 (*br_spacing*) are the basic traits that describe morphology of the branching shapes. Positive
249 correlations between these traits show that in all species in this study the compactness of the
250 colony is preserved. The same relationships between morphological features are also observed
251 in the simulated forms. This supports assumptions made in our computational model that
252 gradients of DIC and light availability in the direct environment of the colony play an
253 important role on the shaping of corals (Merks et.al., 2004; Kaandorp et.al, 2005)

254 In figure 5, samples of the same species group together with few outliers (e.g. *Car436*,
255 *Dec426*, *For421*). However, a better discrimination between the species can be made using
256 multivariate analysis. In the MANOVA-plot in figure 7, we can distinguish two groups: one
257 group are the simulations and the second group consist of the three species *M. carmabi*, *M.*
258 *decactis* and *M. formosa*. *M. mirabilis* lies closer to the simulations except for one sample
259 (*Mir393*). This can be explained by the regular branching pattern of this species. The
260 regularity of the branching patterns is measured by the standard deviation of the branch
261 spacing (*br_spacing*), see histograms in supplementary material. A lower value of the
262 standard deviation indicates a higher regularity. We inspected the linear combinations of
263 variables that form the first two canonical vectors (CVs) in the multivariate analysis
264 (MANOVA). Variables that contributed the most to these vectors were branch thickness (*db*),
265 branching angle (*b_angle*) and branch spacing (*br_spacing*). Therefore, these morphological
266 traits differ the most across the species and simulations.

267 The quantitative validation of our coral growth model demonstrates its ability to
268 simulate a certain group of real corals. The simulated morphologies approximate the
269 morphology of *M. mirabilis* colonies (figure A.7) confirming an earlier study that compared
270 simulated and coral colonies qualitatively (Kaandorp et al., 2005). However, the accretive
271 growth model in its present state is not sufficient to simulate all colony morphologies of the
272 *Madracis* species shown in this analysis. For instance, such morphologies as that of *M.*
273 *formosa* in figure 1d, cannot be generated because of its irregular branching pattern. Some
274 thick branched simulations (*env1_002* in figure 7) also resemble the morphology of *M.*
275 *decactis* colonies.

276 Among model parameters there are two important environmental factors, i.e. light
277 intensity and nutrient source distribution, and one intrinsic factor - nutrient surface
278 redistribution. These factors are known to have an effect on a coral colony morphology (Todd,

279 2008). Hydrodynamics, the structure of individual corallites and inter-polyp communication
280 are not modelled in the present study. Nevertheless, the present study has shown that basic
281 principles of the coral colony morphogenesis can be captured in a computational model. The
282 demonstrated range of simulated shapes (figure 4) can be significantly extended in at least
283 two additional dimensions. First, by incorporating hydrodynamics into the model. And second,
284 by adding physiological or genetic factors that will regulate the growth of a colony from
285 within.

286 Acknowledgements

287

288 This work was funded by the Netherlands Organization for Scientific Research
289 (NWO), VIEW project (# 643100601)

290

291

292 References

293

294 Borgiorni, L., Shafir, S., Angel, D. & B. Rinkevich. 2003. Survival, growth and gonad
295 development of two hermatypic corals subjected to *in situ* fish-farm nutrient enrichment.
296 *Marine Ecology Progress Series* **253**, 137-144.

297

298 Bruno, J.F., & Edmunds, P.J. 1997. Clonal variation for phenotypic plasticity in the coral
299 *Madrasis mirabilis*. *Ecology* **78**, 2177-2190

300

301 Bruno, J.F., & Edmunds, P.J. 1998 Metabolic consequences of phenotypic plasticity in the
302 coral *Madrasis mirabilis* (Duchassaing and Michelotti): the effect of morphology and water
303 flow on aggregate respiration. *Journal of Experimental Marine Biology and Ecology*. 229 ,
304 187 – 195

305

306 Chopard, B. & Droz, M. 1998 Cellular automata modeling of
307 physical systems. Cambridge University Press.

308

309 Diekmann, O.E., Bak R.P.M., Stam W.T. & Olsen J.L. 2001. Molecular genetic evidence for
310 probable reticulate speciation in the coral genus *Madrasis* from Caribbean fringing reef slope.
311 *Marine Biology* **139**, 221-233

- 312
313 Foster, A. B. 1979. Phenotypic plasticity in the reef corals *Montastrea annularis* and
314 *Siderastrea siderea*. *Journal of Experimental Marine Biology and Ecology* **39**, 25-54.
315
- 316 Gattuso, J-P., Allemand, D. & Frankignoulle, M. 1999. Photosynthesis and calcification at
317 cellular, organismal and community levels in coral reefs: A review on interactions and control
318 by carbonate chemistry. *Integrative and Comparative Biology*.
319
- 320 Graus, R.R. and Macintyre, I.G. 1982. Variation in growth forms of the reef *Montastrea*
321 *annularis* (Ellis and Solander): a quantitative evaluation of growth response to light
322 distribution using computer simulation. *Smitson. Contr. Mar. Sci.* 12, 441-464.
323
- 324 Kaandorp, J. A., Sloot, P.M.A., Merks, R.M.H., Bak, R.P.M., Vermeij, M. J. A. & Maier, C.
325 2005. Morphogenesis of the branching reef coral *Madrasis mirabilis*. *Proc. R. Soc. B.* **272**,
326 127-133.
327
- 328 Kaandorp, J.A., & Kübler, J.E. 2001. The algorithmic beauty of seaweeds, sponges and
329 corals. *Mar. Biol.* Heidelberg, Germany: Springer.
330
- 331 Kruszynski, K. J., J. A. Kaandorp, & van Liere, R. 2007. A computational method for
332 quantifying morphological variation in scleractinian corals. *Coral Reefs* **26**, 831-840.
333
- 334 Merks, R.M.H., Hoekstra, A.G., Kaandorp, J.K. & Sloot, P.M.A. 2004. Polyp oriented
335 modelling of coral growth. *J. Theor. Biol.* **228**, 559-576.
336
- 337 Muko, S., Kawasaki, K., Sakai, K., Takasu, F. & Shigesada, N. 2000. Morphological
338 plasticity in the coral *Porites sillimaniani* and its adaptive significance. *Bull. Mar. Sci.* **66**,
339 225-239.
340
- 341 Rosner, B. 1983. Percentage Points for a Generalized ESD Many-Outlier Procedure.
342 *Technometrics*, **25**, 2, 165-172.
343
- 344 Shaish, L., A. Abelson & Rinkevich, B. 2007. How plastic can phenotypic plasticity be? The
345 branching coral *Stylophora pistillata* as a model system. *Plos one* **7**.
346
- 347 Succi, S. 2001 The lattice Boltzmann equation: for fluid dynamics
348 and beyond. Oxford University Press.
349
- 350 Todd, P.A. 2008. Morphological plasticity in scleractinian corals. *Biol. Rev.* **83**, 315-337.
351
- 352 Todd P.A., Sidle R.C., Lewin-Koh N.J.I. 2004. An aquarium experiment for identifying the
353 physical factors inducing morphological change in two massive scleractinian corals. *Journal*
354 *of Experimental Marine Biology and Ecology*.
355
- 356 Veron, J.E.N., 1995. Corals in Space and Time: The Biogeography and Evolution of the
357 Scleractinia. UNSW
358 Press, Sydney, Australia.
359

360 Willis, B. L. 1985. Phenotypic plasticity versus phenotypic tability in the reef corals
361 *Turbinaria mesenteria* and *Pavona Cactus*. *Proceedings of the Fifth International Coral Reef*
362 *Congress* 4, 107-112.

363
364 Wallace, C.C. 1999. Staghorn corals of the world: a revision of the genus *Acropora*, CSIRO,
365 Collingwood.

366
367
368

369 **Figures**

370
371 Figure 1.
372 Volume rendering of the CT-scans of real coral colonies.

373
374 Figure 2.
375 a) Morphological skeleton generated from a volume, b) branch thickness, da – white sphere,
376 db – black sphere, dc – gray sphere, c) branch spacing (*br-spacing*) and d) branching angle
377 relative to the growth direction (g_angle).

378
379
380 Figure 3.
381 Simulation setup. A growing object bounded by the simulation box with a source plane on the
382 top and the substrate plane at the bottom.

383
384
385
386 Figure 4.
387 Morphospace of simulated coral colonies in two different environments: a) nutrients
388 source is above the object, i.e. mimicking the presence of competing colonies near the
389 simulated colony, b) side planes act also as the nutrient sources, i.e. mimicking the absence of
390 competing colonies near the simulated colony. The axes represent parameters, which can be
391 gradually changed in order to change colony morphology. Light
392 intensity is the a parameter from equation 2.1. Surface diffusion is the diffusion constant
393 D in equation 2.2.

394
395 Figure 5.
396 A scatter plot of the correlation between branch thickness (db) and branch spacing
397 ($br_spacing$). In colored labels of real corals the first three characters denote the name of the
398 species, i.e. Mir $\equiv M. mirabilis$, For $\equiv M. formosa$, Dec $\equiv M. decactis$ and Car $\equiv M. carmabi$.
399 Followed by the id-number in our coral database. Simulated growth form are denoted using
400 black labels, where the simulated environment ($env1$ – one source plane or $env4$ – four
401 additional source planes) is followed by the value of surface diffusion coefficient. In
402 simulations where the influence of light is taken into account ($light1$) the value of the surface
403 diffusion coefficient is followed by the value of light intensity parameter.

404
405 Figure 6.
406 Scatter plot of the first two principal components. For the labels description see caption figure
407 5.

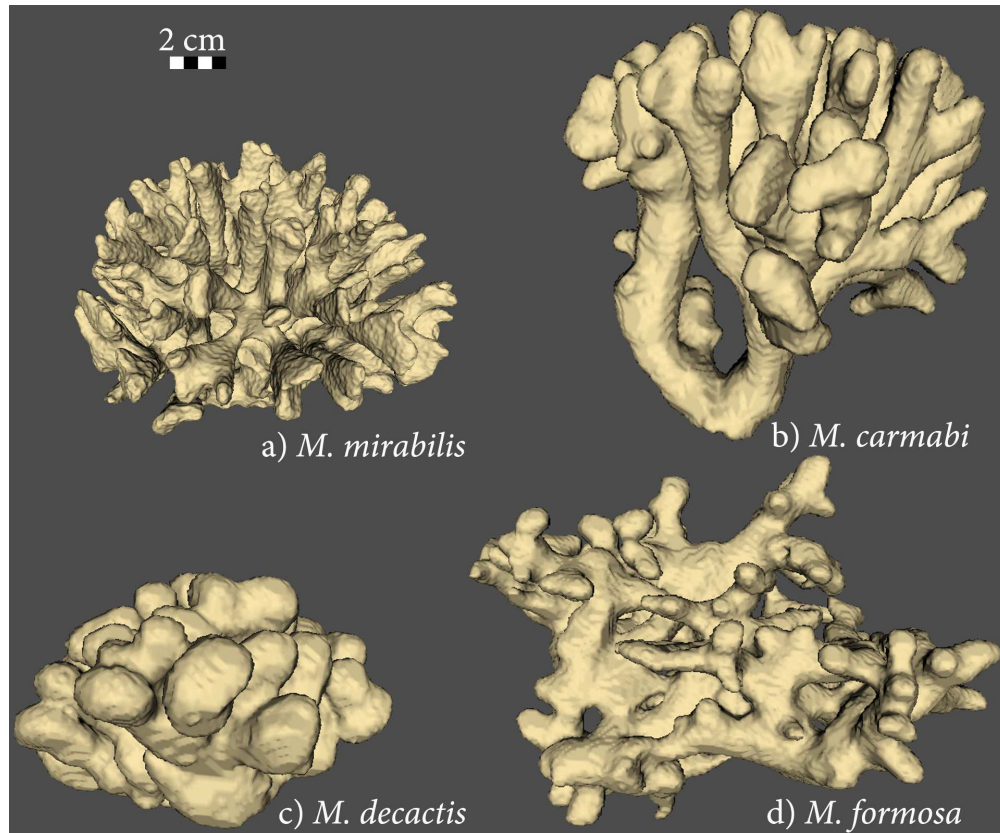
408

409 Figure 7.

410 MANOVA plot of the first two canonical vectors (CVs). For the labels description see caption

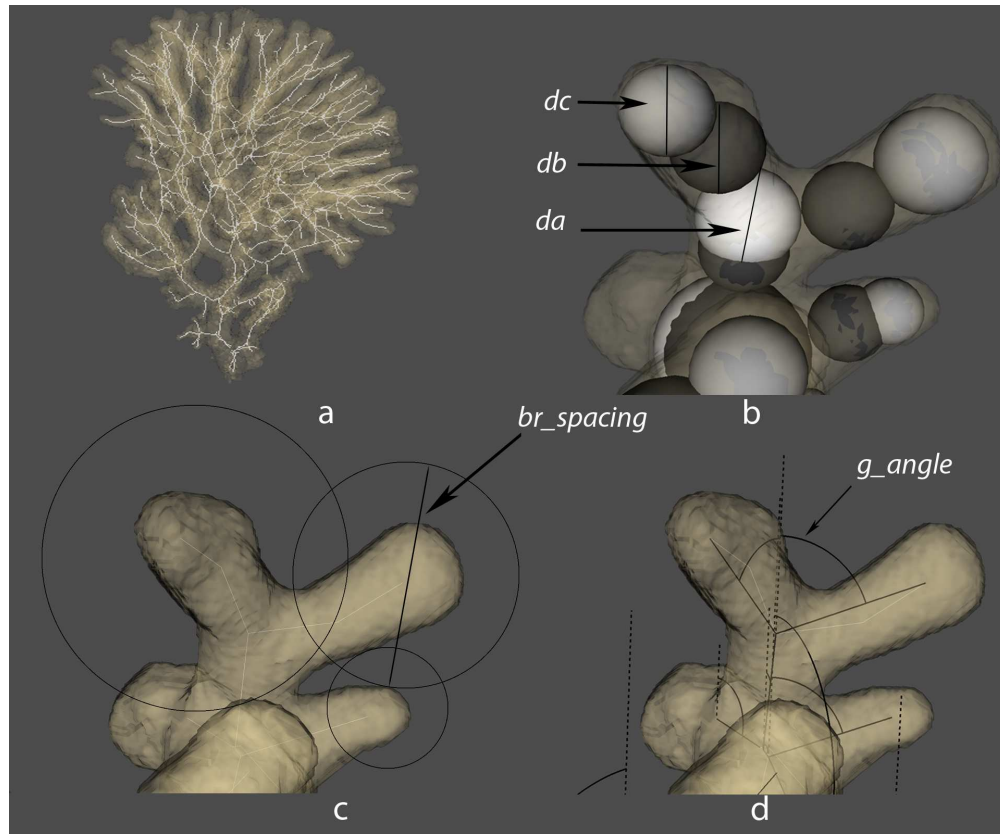
411 figure 5.

For Review Only

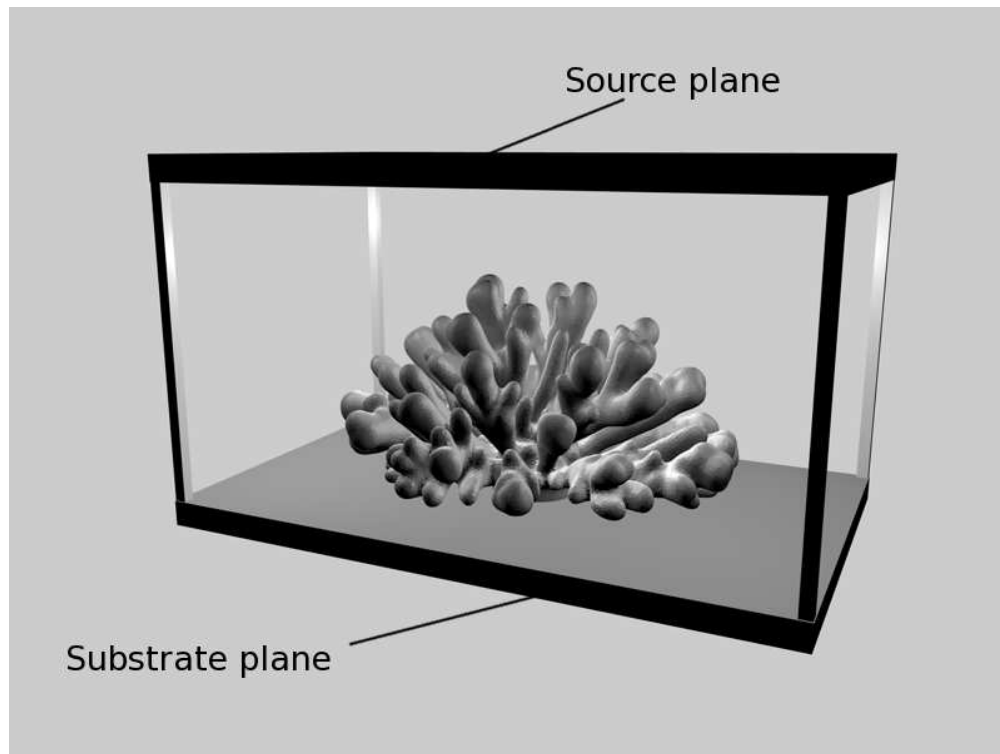


Volume rendering of the CT-scans of real coral colonies.
121x101mm (400 x 400 DPI)

Only

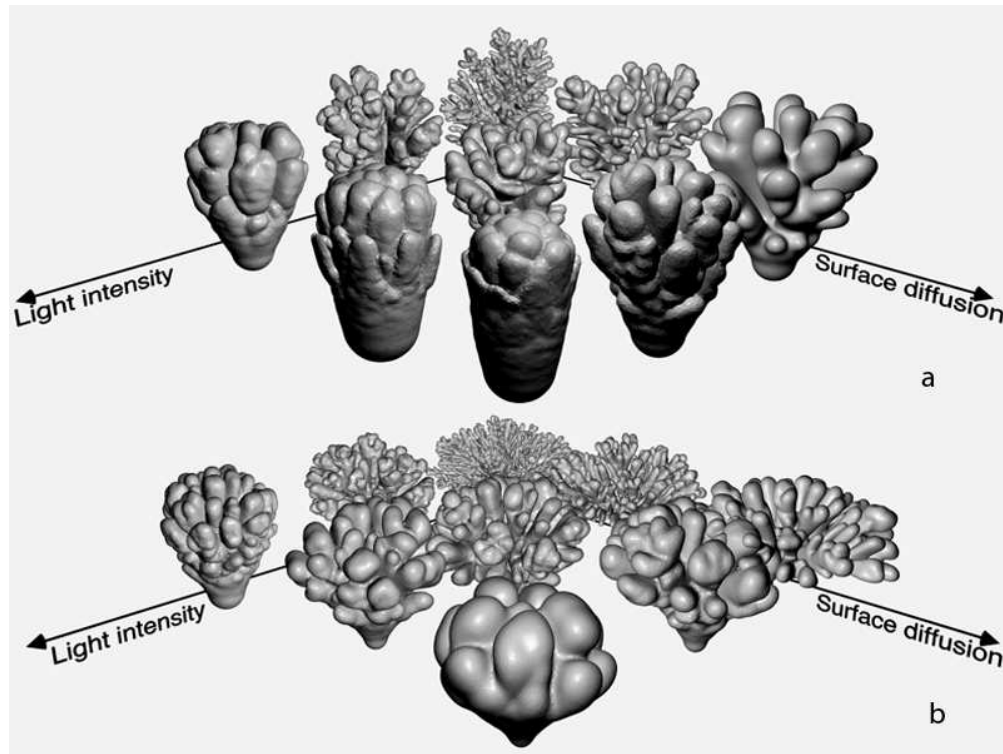


a) Morphological skeleton generated from a volume, b) branch thickness, *da* – white sphere, *db* – black sphere, *dc* – gray sphere, c) branch spacing (*br-spacing*) and d) branching angle relative to the growth direction (*g_angle*).
121x101mm (400 x 400 DPI)



Simulation setup. A growing object bounded by the simulation box with a source plane on the top and the substrate plane at the bottom.
67x50mm (300 x 300 DPI)

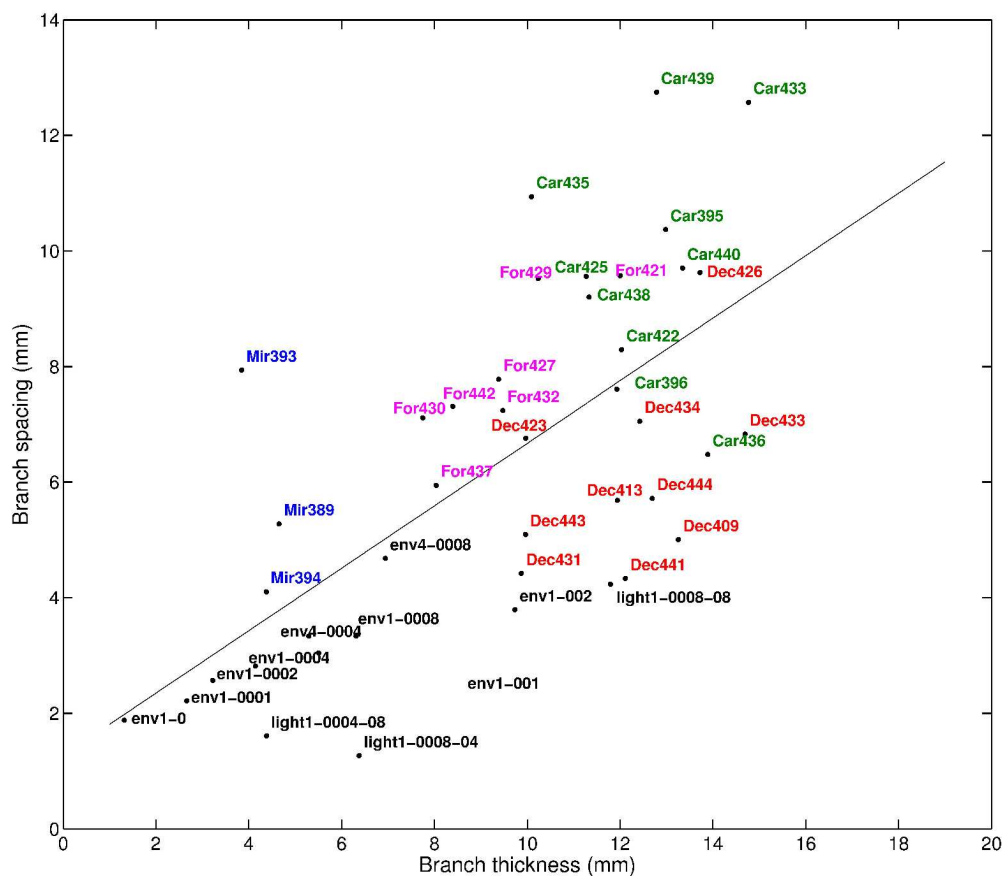
Only



Morphospace of simulated coral colonies in two different environments: a) nutrients source is above the object, i.e. mimicking the presence of competing colonies near the simulated colony, b) side planes act also as the nutrient sources, i.e. mimicking the absence of competing colonies near the simulated colony. The axes represent parameters, which can be gradually changed in order to change colony morphology. Light intensity is the a parameter from equation 2.1. Surface diffusion is the diffusion constant D in equation 2.2.

67x50mm (300 x 300 DPI)





A scatter plot of the correlation between branch thickness (db) and branch spacing (br_spacing). In colored labels of real corals the first three characters denote the name of the species, i.e. Mir \equiv M. mirabilis, For \equiv M. formosa, Dec \equiv M. decactis and Car \equiv M. carmabi. Followed by the id-number in our coral database. Simulated growth form are denoted using black labels, where the simulated environment (env1 – one source plane or env4 – four additional source planes) is followed by the value of surface diffusion coefficient. In simulations where the influence of light is taken into account (light1) the value of the surface diffusion coefficient is followed by the value of light intensity parameter.

265x232mm (600 x 600 DPI)

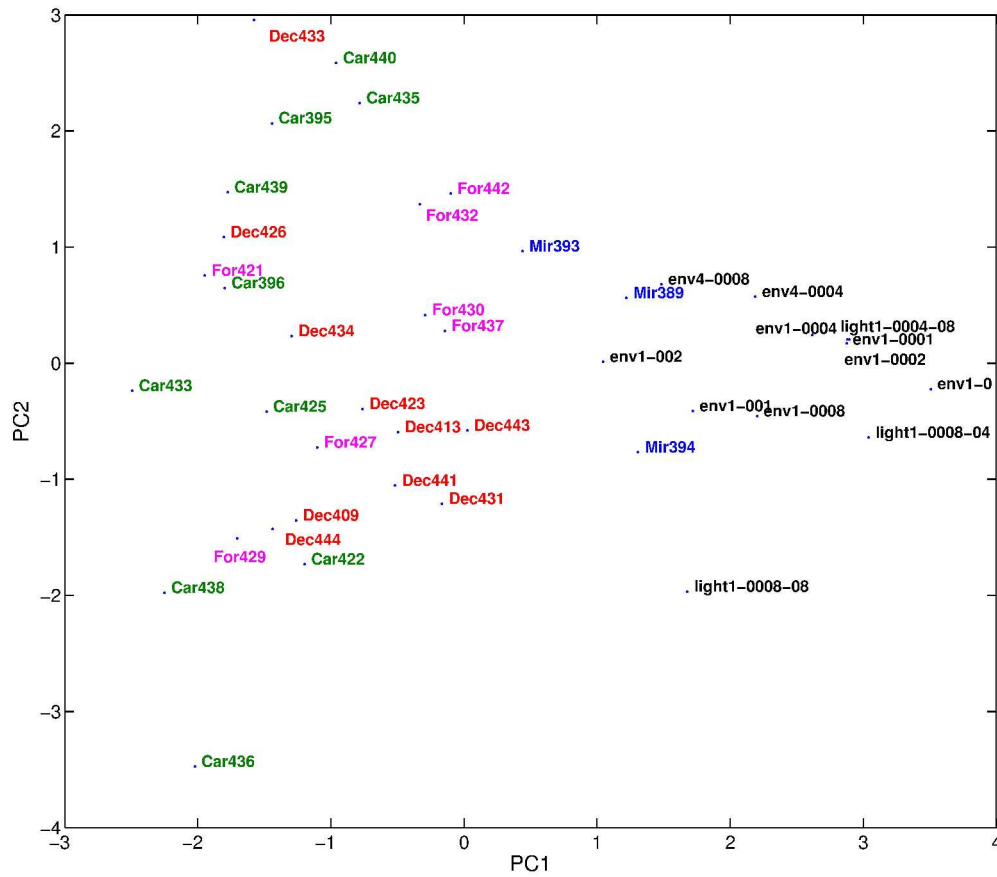
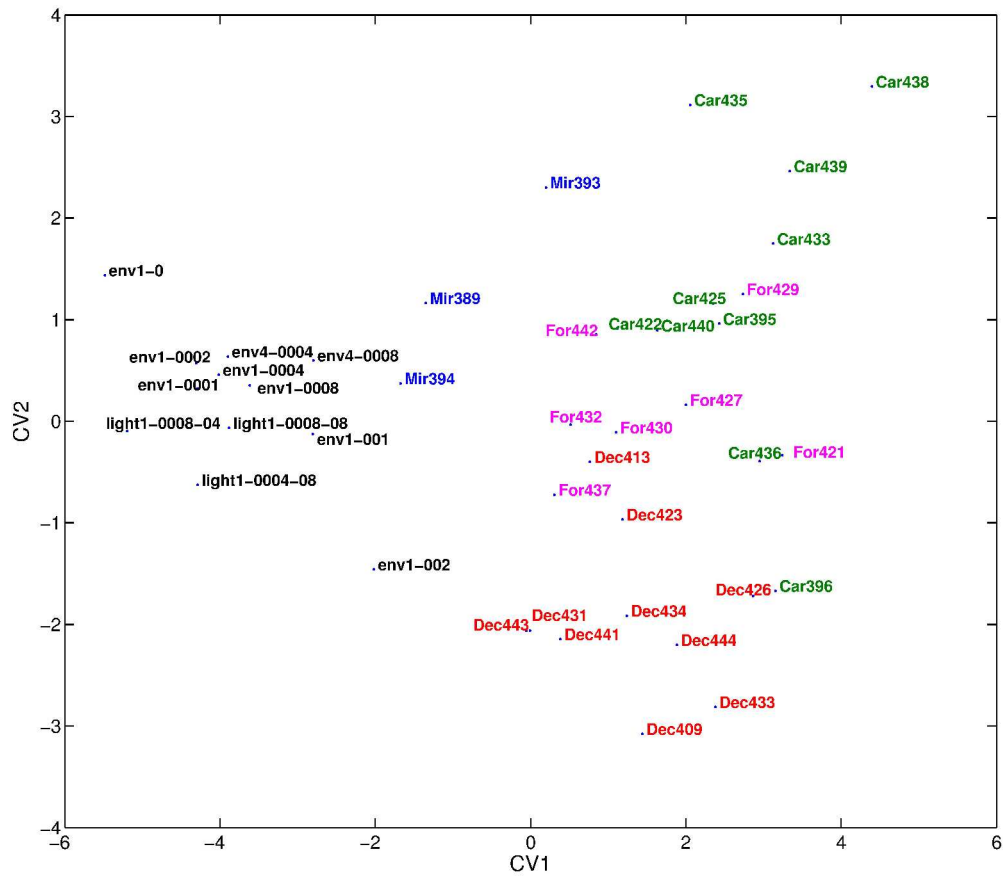


Figure 6.
Scatter plot of the first two principal components. For the labels description see caption figure 5.

264x232mm (600 x 600 DPI)





MANOVA plot of the first two canonical vectors (CVs). For the labels description see caption figure 5.
264x232mm (600 x 600 DPI)